Fundamental coarse space components for Schwarz methods with crosspoints

François Cuvelier and Martin J. Gander and Laurence Halpern

1 Introduction

Historically, coarse spaces for domain decomposition methods were based on a coarse grid, like in geometric multigrid methods, see e.g. [17, page 36]: "The subspace V_0 is usually related to a coarse problem, often built on a coarse mesh". More recently, a wealth of research has been devoted to design new coarse spaces for high contrast problems: after first steps in [3, 13], where volume eigenfunctions were used, see also [2], a coarse space using the eigenfunctions of the Dirichlet-to-Neumann maps on the boundary of each subdomain was developed in [15, 1]. This then led to the GenEO coarse space [16], and also motivated the ACMS based coarse space [11], all seminal for many further developments: for FETI, see for example [14], or for the GDSW coarse space, see [12]. A different idea for new coarse spaces is to first define an optimal coarse space, which makes the method a direct solver [6, 7], and then to approximate it, which led to the SHEM coarse space [8, 9, 10, 4].

Our new idea here is to design a coarse space based on insight from the eigenmodes of the parallel Schwarz iteration operator that converge most slowly. We start with a numerical experiment for Laplace's equation on the unit square divided into 4×4 subdomains using the classical parallel Schwarz method of Lions with minimal overlap[1]. In Figure 1 we observe that the error in the iteration, after an initial transient phase, forms two typical distinct

François Cuvelier
LAGA, Université Sorbonne Paris-Nord, e-mail: cuvelier@math.univ-paris13.fr

Martin J. Gander
Section de Mathématiques, Université de Genève, e-mail: martin.gander@unige.ch

Laurence Halpern
LAGA, Université Sorbonne Paris-Nord, e-mail: halpern@math.univ-paris13.fr

[1] With minimal overlap (and only then) this is equivalent to Additive Schwarz without Conjugate Gradient acceleration.
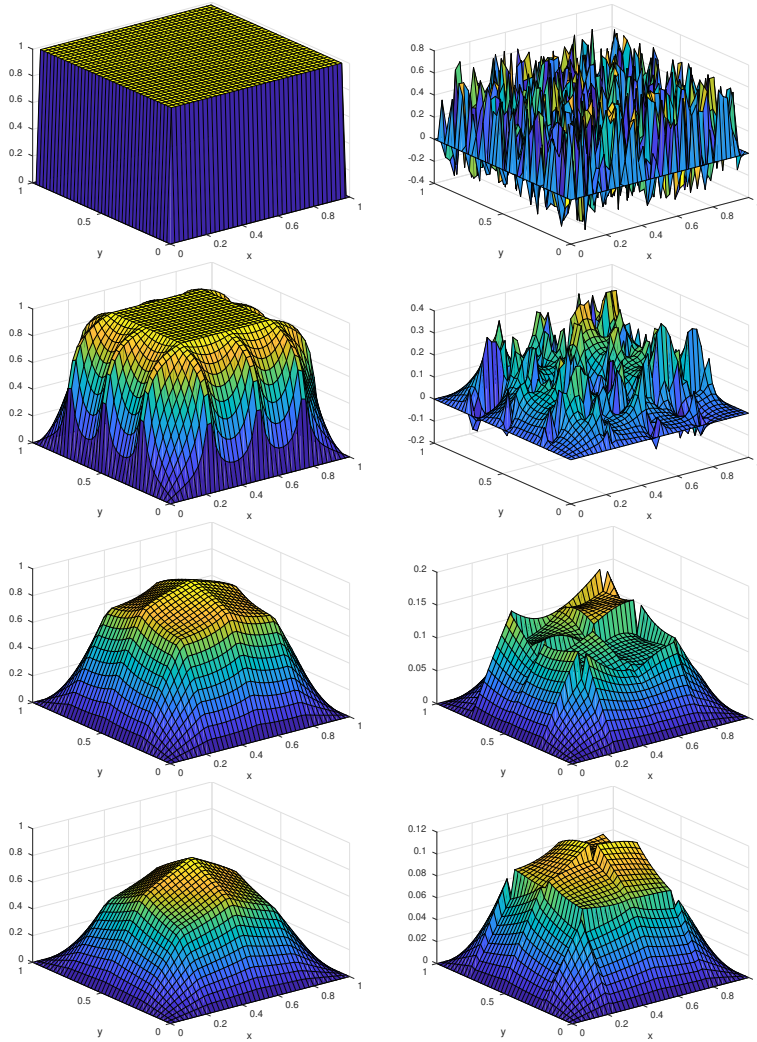
Fig. 1: Error for the parallel Schwarz method of Lions with 4×4 subdomains at iteration $0, 1, 10, 20$ from top to bottom. Left: constant initial error, Right: random initial error.

modes which converge most slowly: for the constant initial guess we see a continuous mode consisting of affine (harmonic) functions in each subdomain, whereas for the random initial guess these functions seem to be discontinuous across subdomains. Our goal is to understand this behavior by studying the eigenmodes of the continuous parallel Schwarz iteration operator, and to deduce from this study a very effective new coarse space for Schwarz methods.
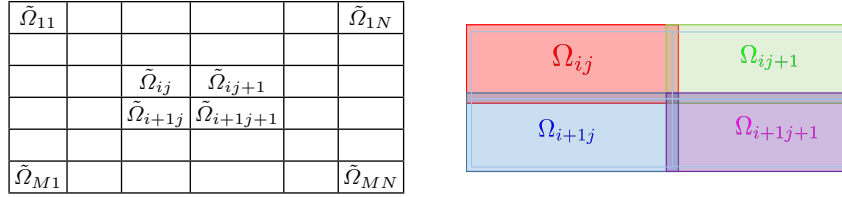
Fig. 2: Left: general decomposition of a rectangle into $M \times N$ subrectangles $\tilde{\Omega}_{ij}$. Right: adding $2L$ overlap to obtain the subdomains Ω_{ij}.

2 Modal analysis of the Schwarz iteration map

We consider a general decomposition of a rectangle into $M \times N$ smaller overlapping rectangles Ω_{ij}, as indicated in Figure 2. We denote by (x_j, y_i) the crosspoints of the nonoverlapping decomposition. The parallel Schwarz iteration from $\prod H^1(\Omega_{ij})$ into itself maps the old error iterate $u = \{u_{ij}\}$ which is harmonic in the subdomains, into a new error $v = \{v_{ij}\}$, also harmonic in the subdomains. We allow in our analysis the more general Robin transmission conditions, which on the vertical interfaces are

$$
\begin{aligned}
\partial_x v_{ij} + p v_{ij} &= \partial_x u_{ij+1} + p u_{ij+1}, \quad x = x_j + L, \\
-\partial_x v_{ij+1} + p v_{ij+1} &= -\partial_x u_{ij} + p u_{ij}, \quad x = x_j - L,
\end{aligned}
$$

and similarly on the horizontal interfaces at $y_i \pm L$. For $p = +\infty$ and $L > 0$, our results will correspond to the classical parallel Schwarz method of Lions with Dirichlet transmission conditions. If $0 < p < +\infty$ and $L \geq 0$, our results will correspond to a possibly non-overlapping optimized parallel Schwarz method.

An eigenmode of the iteration map associated to an eigenvalue λ is defined by $v = \lambda u$, λ being the convergence factor of this mode. For simplicity, we study the case where all underlying nonoverlapping subdomains are squares of equal sides H. The error function u_{ij} in the subdomain Ω_{ij} is harmonic, and we use separation of variables,

$$
u_{ij} = (a_{ij} \sin \zeta(x - x_{j-1}) + a'_{ij} \sin \zeta(x - x_j))(b_{ij} \sinh \zeta(y - y_{i-1}) + b'_{ij} \sinh \zeta(y - y_i))
$$

for the oscillatory modes in x. Exchanging x and y gives the oscillatory modes in y. Affine modes are obtained by replacing $\sin \zeta(x - x_{j-1})$ by $(x - x_{j-1})$ for instance. By a lengthy, technical computation, we obtain

Theorem 1 (Eigenvalue-Frequency Relation)

Defining for each $\zeta \neq 0$ the quantities

$$Z^- := \zeta \cos \zeta (H-L) - p \sin \zeta (H-L), \; Z_h^- := \zeta \cosh \zeta (H-L) - p \sinh \zeta (H-L),$$
$$Z^+ := \zeta \cos \zeta (H+L) + p \sin \zeta (H+L), \; Z_h^+ := \zeta \cosh \zeta (H+L) + p \sinh \zeta (H+L),$$
$$Z^0 := \zeta \cos \zeta L + p \sin \zeta L, \qquad\qquad Z_h^0 := \zeta \cosh \zeta L + p \sinh \zeta L,$$

the eigenvalue λ, the angular frequency ζ and the coefficients of the eigenmode are related by

$$
\begin{aligned}
\lambda(Z^+ + \delta_x^{(j)} Z^0)a_{ij}b_{ij} &= (Z^0 + \delta_x^{(j+1)} Z^-)a_{ij+1}b_{ij+1}, \\
\lambda(Z^0 + \delta_x^{(j+1)} Z^+)a_{ij+1}b_{ij+1} &= (Z^- + \delta_x^{(j)} Z^0)a_{ij}b_{ij}, \\
\lambda(Z_h^+ + \delta_y^{(i)} Z_h^0)a_{ij}b_{ij} &= (Z_h^0 + \delta_y^{(i+1)} Z_h^-)a_{i+1j}b_{i+1j}, \\
\lambda(Z_h^0 + \delta_y^{(i+1)} Z_h^+)a_{i+1j}b_{i+1j} &= (Z_h^- + \delta_y^{(i)} Z_h^0)a_{ij}b_{ij},
\end{aligned}
\tag{1}
$$

where the numbers $\delta_x^{(j)} := \frac{a'_{ij}}{a_{ij}}$ and $\delta_y^{(i)} := \frac{b'_{ij}}{b_{ij}}$ for $j = 1, \ldots N-1$ and $i = 1, \ldots M-1$.

The dispersion relation (equation for the modes) is obtained from (1) by multiplying pairwise the equations, which leads to

Theorem 2 (Eigenvalues of the $M \times N$ Schwarz iteration map)

$$
\begin{aligned}
\lambda^2 &= \frac{Z^- + \delta_x^{(j)} Z^0}{Z^+ + \delta_x^{(j)} Z^0} \frac{Z^0 + \delta_x^{(j+1)} Z^-}{Z^0 + \delta_x^{(j+1)} Z^+}, \quad j = 1 \ldots N-1, \\
\lambda^2 &= \frac{Z_h^- + \delta_y^{(i)} Z_h^0}{Z_h^+ + \delta_y^{(i)} Z_h^0} \frac{Z_h^0 + \delta_y^{(i+1)} Z_h^-}{Z_h^0 + \delta_y^{(i+1)} Z_h^+}, \quad i = 1 \ldots M-1.
\end{aligned}
\tag{2}
$$

With Theorem 1 and Theorem 2, we thus have a complete characterization of the eigenmodes of the classical and optimized parallel Schwarz iteration map for decompositions of the form in Figure 2 for squares. The affine modes, some of which we observed in the numerical experiment in Figure 1, are obtained by letting ζ go to zero in (2), and we obtain by a direct calculation

Corollary 1 (Existence of affine Eigenmodes) *For $N \times N$ subdomains, there are $2(N-1)$ affine modes. There are no affine modes when $M \neq N$.*

For our initial experiment setting, $N = M = 4$, there are 6 affine eigenmodes, shown in Figure 3 for $p = 10^{15}$ to emulate classical parallel Schwarz, and overlap $L = 0.1$. We clearly recognize on the top left the slowest eigenmode we saw in the numerical experiment in Figure 1 on the left. We also see a corresponding discontinuous eigenmode just below on the left in Figure 3, responsible for the same slow convergence in our numerical experiment in Figure 1 on the right, since their eigenvalues are equal in modulus. It is therefore important for a good coarse space for Schwarz methods to contain both continuous and discontinuous harmonic functions per subdomain.
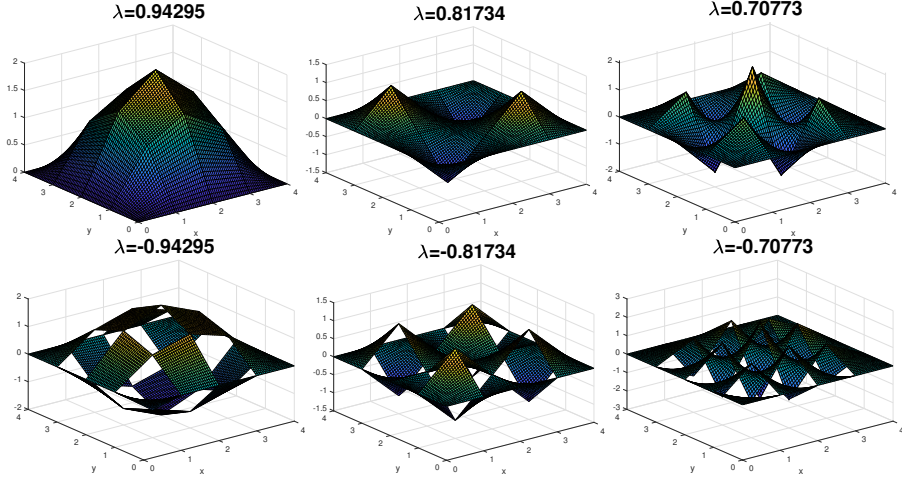
Fig. 3: Affine eigenmodes for 4×4 subdomains.
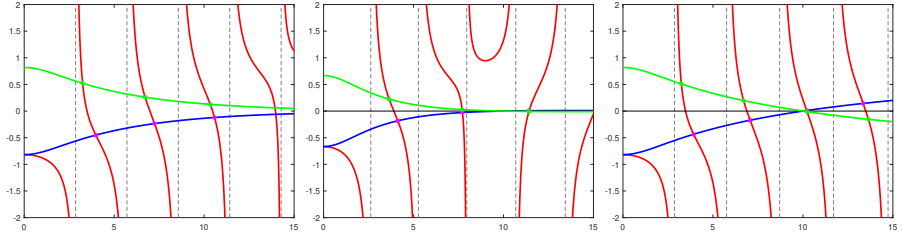
Fig. 4: Functions φ in red, φ_h in green and $-\varphi_h$ in blue. Left: classical parallel Schwarz method of Lions. Middle: overlapping optimized Schwarz. Right: Nonoverlapping optimized Schwarz.

3 The special case of 2×2 subdomains

For a 2×2 domain decomposition, the relation (2) between λ and ζ takes the simple form

$$\lambda^2 = \left(\varphi(\zeta)\right)^2 = \left(\varphi_h(\zeta)\right)^2, \quad \varphi(\zeta) = \frac{Z^-}{Z^+}(\zeta), \ \varphi_h(\zeta) = \frac{Z_h^-}{Z_h^+}(\zeta). \qquad (3)$$

Then ζ is determine by either choosing the positive or negative sign,

$$\varphi(\zeta) = \varphi_h(\zeta), \qquad \varphi(\zeta) = -\varphi_h(\zeta). \qquad (4)$$

Each of these equations has a sequence of solutions we denote by $\zeta_1^k(p, H, L)$ and $\zeta_2^k(p, H, L)$. We show in Figure 4 these functions of ζ, and intersections represent thus solutions of (4). We chose subdomain length $H = 1$, and,
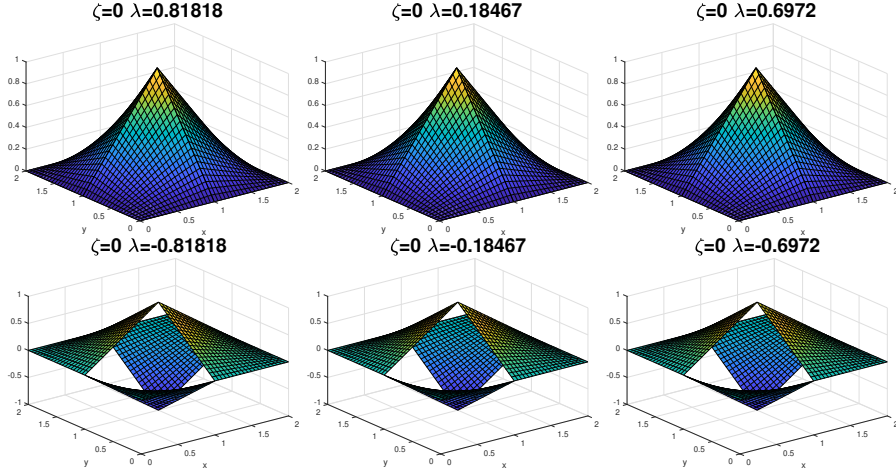
Fig. 5: Slowest, affine eigenmodes. Left: classical parallel Schwarz method of Lions. Middle: overlapping optimized Schwarz. Right: nonoverlapping optimized Schwarz.

if present, for the overlap $L = 0.1$ and the Robin parameter $p = 10$. The frequencies $\zeta_1^k(p, H, L)$ are at the intersection between the red and the green curve, while the frequencies $\zeta_2^k(p, H, L)$ are at the intersection between the red and the blue curve. The value of any of the functions at those points represents a corresponding eigenvalue λ of the Schwarz iteration map.

In Figure 5 we show the two affine eigenmodes, at the top the continuous and the bottom the discontinuous ones, corresponding to $\zeta = 0$ in (4), together with the corresponding λ for all three Schwarz variants. These are the most slowly converging modes, and their corresponding eigenvalues in modulus show that the three different parallel Schwarz variants have very different convergence speeds: classical parallel Schwarz method of Lions on the left converges most slowly, while optimized Schwarz with overlap in the middle is the fastest, followed by optimized Schwarz without overlap. The affine eigenmodes in Figure 5 look however very similar for all three Schwarz variants, an observation which is the basis for our new coarse space for Schwarz methods.

4 A new coarse space for parallel Schwarz methods

The affine eigenmodes in Figure 5 do not only look very similar, they are asymptotically the same, and the following theorem shows that they are the basis to assemble such affine eigenfunctions for more general N.

Theorem 3 (Asymptotic Assembly Theorem) *When the overlap L is small, and/or the Robin parameter p is large, the affine modes for $N \times N$ subdomains are asymptotically special linear combinations of the two limiting affine functions Θ^c and Θ^d from the 2×2 decomposition modulo translations.*

For our initial 4×4 subdomain example, the precise asymptotic formulas, with respect to $X = \frac{H}{L}$ (classical parallel Schwarz method of Lions) or $X = pH$ (optimized Schwarz), are for the eigenvalues, with $\varepsilon = \pm 1$,

$$\lambda^{(1),\varepsilon} \sim \varepsilon(1 - \frac{2 + \sqrt{2}}{X}), \quad \lambda^{(2),\varepsilon} \sim \varepsilon(1 - \frac{2}{X}), \quad \lambda^{(3),\varepsilon} \sim \varepsilon(1 - \frac{2 - \sqrt{2}}{X}),$$

and for the corresponding six eigenfunctions shown in Figure 3 we have

$$
\begin{aligned}
u^{(1),1} &\sim \Theta^c_{11} + \Theta^c_{13} + \Theta^c_{31} + \Theta^c_{33} + \sqrt{2}(\Theta^c_{12} + \Theta^c_{21} + \Theta^c_{23} + \Theta^c_{32}) + 2\Theta^d_{22}, \\
u^{(1),-1} &\sim \Theta^d_{11} + \Theta^d_{13} + \Theta^d_{31} + \Theta^d_{33} - \sqrt{2}(\Theta^d_{12} + \Theta^d_{21} + \Theta^d_{23} + \Theta^d_{32}) + 2\Theta^d_{22}, \\
u^{(2),1} &\sim \Theta^c_{11} - \Theta^c_{13} - \Theta^c_{31} + \Theta^c_{33}, \\
u^{(2),-1} &\sim \Theta^d_{11} - \Theta^d_{13} - \Theta^d_{31} + \Theta^d_{33}, \\
u^{(3),1} &\sim \Theta^c_{11} + \Theta^c_{13} + \Theta^c_{31} + \Theta^c_{33} - \sqrt{2}(\Theta^c_{12} + \Theta^c_{21} + \Theta^c_{23} + \Theta^c_{32}) + 2\Theta^c_{22}, \\
u^{(3),-1} &\sim \Theta^d_{11} + \Theta^d_{13} + \Theta^d_{31} + \Theta^d_{33} + \sqrt{2}(\Theta^d_{12} + \Theta^d_{21} + \Theta^d_{23} + \Theta^d_{32}) + 2\Theta^d_{22}.
\end{aligned}
$$

We therefore propose a new coarse space for Schwarz methods, based on assembling the continuous and discontinuous 'hat' functions Θ^c_{ij} and Θ^d_{ij} from the 2×2 subdomain decomposition, as illustrated for our example in Figure 6. We allow our new two-level Schwarz methods also to perform more than just $\nu = 1$ domain decomposition iteration or smoothing step, since the new coarse space is so effective that it does not need to be used at every iteration, as we will see in the next section.

5 Numerical experiments

We start with a numerical experiment for our 4×4 example, running a nonoverlapping optimized Schwarz method (OSM) to solve Laplace's equation using now a finite element discretization, as indicated in Figure 7 on the left. On the right, we show how the error decreases, both for the one-level OSM and 2-level-OSM with two different numbers of smoothing steps $\nu = 1, 4$. We see that it is sufficient to use a coarse correction with our new coarse space only every fourth Schwarz iteration with a two-level optimized parameter $p_{\text{opt}} = 50.3$, and this value is very different from the one-level optimized parameter $p_{\text{opt}} = 14.1$, as one can see from the one-level convergence curves, see also Section 6.

We next show a numerical experiment for a more general decomposition obtained by METIS, shown in Figure 8. Here we constructed our new coarse space by generating harmonic functions in the subdomains from edge solu-
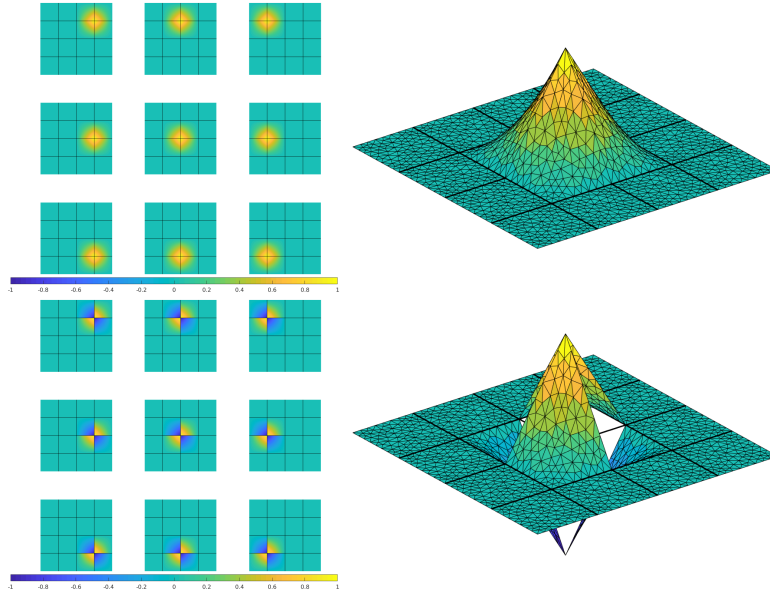
Fig. 6: Our new coarse space assembly for 4×4 subdomains. Top: continuous functions Θ_{ij}^c. Bottom: discontinuous functions Θ_{ij}^d.
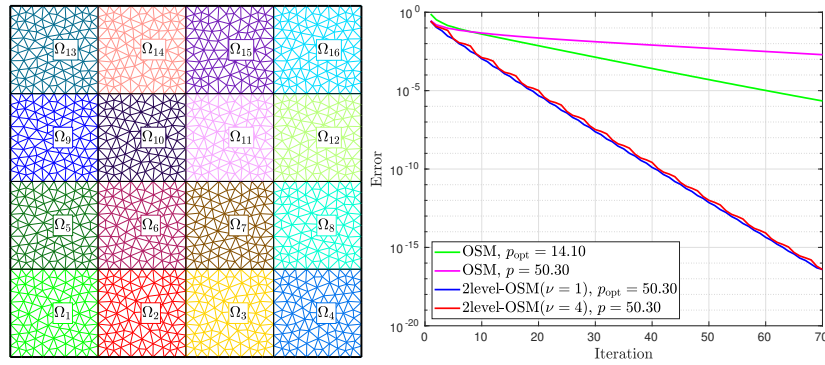

Fig. 7: Left: finite element setting for our 4×4 model problem. Right: convergence comparison of the one- and two-level optimized Schwarz methods.

tions of the Laplace-Beltrami operator, and we span both continuous and discontinuous 'hat' functions as in the rectangular decomposition. For cross points with an even number of incoming edges, we need again two functions, one continuous and one discontinuous, like in the rectangular case, and for cross points with an odd number of incoming edges, we need three functions, one continuous and two discontinuous ones, except when only 3 edges are incoming, for which case one continuous coarse function suffices! We see again
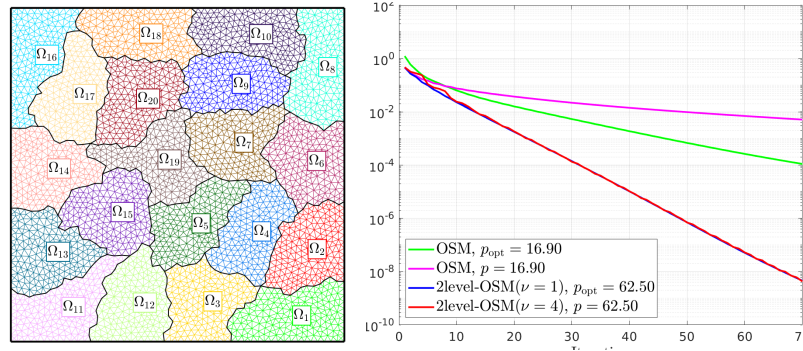
Fig. 8: Left: finite element example obtained from METIS. Right: convergence comparison of the one- and two-level optimized Schwarz methods.
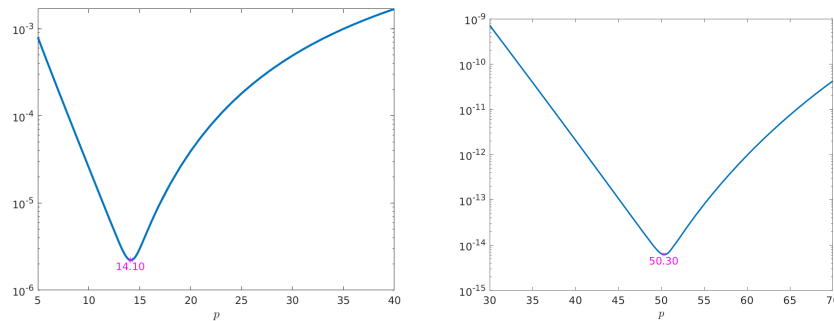

Fig. 9: Left: one-level OSM after 70 iterations. Right: two-level OSM with $\nu = 1$ after 60 iterations (since `macheps` is already reached).

a similar behavior in the convergence of the optimized new two-level Schwarz method, and a coarse correction every fourth iteration suffices with our new coarse space.

6 A note on the optimized Robin parameter

From the literature on optimized Schwarz methods, the optimized choice of the Robin parameter is known from two subdomain analysis [5], e.g. in the non-overlapping case $p^* \sim \frac{\pi}{\sqrt{Hh}}$. In the case with cross points, there are no results available so far. We first show a numerical experiment for our 4×4 original model problem from Figure 7 running the method for many values of the parameter p, and plotting the error as a function of p, see Figure 9. We clearly see that in both cases there is a best parameter p^*. This parameter is
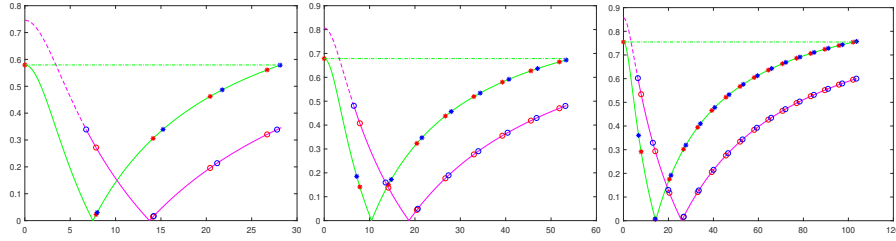
Fig. 10: Convergence factors $|\varphi_h(\zeta)|$ of our optimized Schwarz methods for $h = 1/2^4, 1/2^5, 1/2^6$ from left to right. Green-star: one level, magental-circle: two level method

$p_1^* = 14.1$ for the one-level method, and $p_2^* = 50.3$ for the two-level method, also used in Figure 7.

In order to better understand this optimized choice, we return to the optimization of the convergence factor for 2×2 subdomains. Recall that the relevant frequencies ζ_j^k are a discrete set, defined in (4). We show in Figure 10 the convergence factor, $|\lambda| = \left| \frac{Z_h^-}{Z_h^+} \right|$ as a function of ζ, for our optimized Schwarz method, $H = 1/2$ and three different fine mesh parameters h. Best performance in optimized Schwarz methods is obtained by equioscillation in the convergence factor [5], in the non-overlapping case between the lowest and highest frequency (green curves in Figure 10). Since our new coarse space with affine modes removes the lowest frequency, the best parameter choice now only needs to equioscillate with the second lowest and the highest frequency (magenta curves in Figure 10), which explains why p^* for the two-level method with our new coarse space is larger than p^* for the one-level method. One can show that for given H and h, the highest frequency index is $k_0 = \frac{1}{2} \frac{H}{h} + 1$, and equating the values of $|\varphi_h(\zeta)|$ at $\zeta = 0$ and $\zeta = \zeta_2(k_0, p)$ gives the optimized parameter p_1^* for the one-level method. For the two-level method, equating the values of $|\varphi_h(\zeta)|$ at $\zeta = \zeta_2(1, p)$ and $\zeta = \zeta_2(k_0, p)$ yields the optimized value p_2^* for the two-level method. An asymptotic analysis gives

$$p_1^* \sim \sqrt{\frac{\pi}{2Hh}}, \quad p_2^* \sim \pi \sqrt{\frac{\coth \pi}{2Hh}}, \quad p^* \sim \pi \sqrt{\frac{\coth \pi}{Hh}}, \tag{5}$$

where p^* is the best parameter obtained for two subdomains. Naturally we can enrich our new coarse space with the next, non-affine modes that come in the Schwarz iteration spectrum, which we show in Figure 11 (the corresponding ones exchanging x and y are not shown), and then the optimized parameter would again increase further when an OSM is used. We see that these modes are very similar to the SHEM modes, but again they come in pairs, thus reducing the SHEM coarse space dimension by a factor of two. We see however also specific new modes appear, like the ones in the top row of Figure 11 which
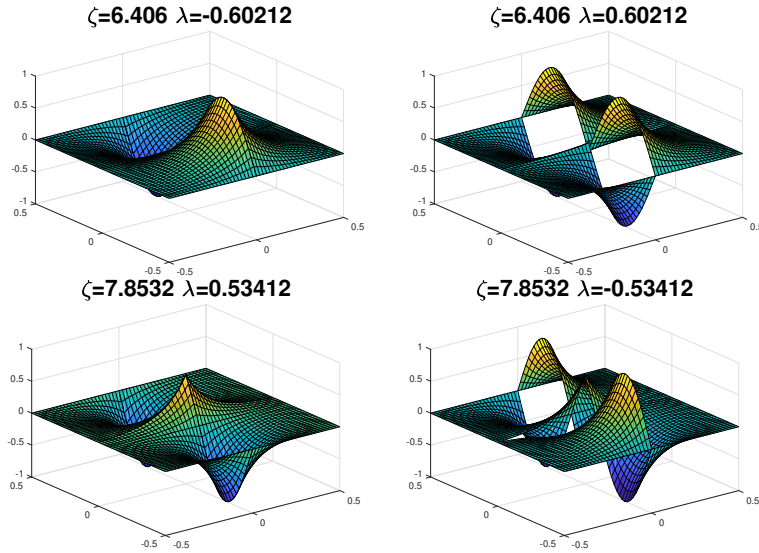
Fig. 11: First non affine modes to enrich our new coarse space.

form a tip at the cross point, and were not in the spectral sine decomposition of the SHEM coarse space, an issue which merits further investigation.

7 Conclusion

We designed a new coarse space for Schwarz methods, based on a spectral analysis of the parallel Schwarz iteration operator. Our new coarse space is assembled from continuous and discontinuous hat functions obtained from the eigenfunctions of local 2×2 subdomain decompositions. The new coarse space components are the same for the classical parallel Schwarz method of Lions, and overlapping and non-overlapping optimized Schwarz. We showed numerically that our new coarse space is also very effective on more general decompositions, like the ones obtained by METIS, and that using a coarse space modifies in an important way the optimized parameter in the Robin transmission conditions of the optimized Schwarz methods. Further enrichment is possible with known oscillatory enrichment functions, again from the analysis of local 2×2 subdomain decompositions.

Clearly our work is just a first step for the construction of such type of new coarse spaces. Our approach can be used to detect good coarse space components for other types of partial differential equations, like problems with high contrast, advection diffusion problems, or also the much harder case of time harmonic wave propagation. This is possible also for situations where

there is no general convergence theory for the associated Schwarz method available, since it is based on a direct spectral study of the Schwarz iteration operator in a simplified setting.

References

1. V. Dolean, F. Nataf, R. Scheichl, and N. Spillane. Analysis of a two-level Schwarz method with coarse spaces based on local Dirichlet-to-Neumann maps. *Comput. Methods Appl. Math.*, 12(4):391–414, 2012.
2. Y. Efendiev, J. Galvis, R. Lazarov, and J. Willems. Robust domain decomposition preconditioners for abstract symmetric positive definite bilinear forms. *ESAIM: Math. Model. Numer. Anal.*, 46(5):1175–1199, 2012.
3. J. Galvis and Y. Efendiev. Domain decomposition preconditioners for multiscale flows in high-contrast media. *Multiscale Model. Simul.*, 8(4):1461–1483, 2010.
4. Martin J. Gander and Bo Song. Complete, optimal and optimized coarse spaces for additive Schwarz. In *Domain Decomposition Methods in Science and Engineering XXIV*, pages 301–309, 2019.
5. M.J. Gander. Optimized Schwarz methods. *SIAM J. Numer. Anal.*, 44(2):699–731, 2006.
6. M.J. Gander and L. Halpern. Méthode de décomposition de domaine. *Encyclopédie électronique pour les ingénieurs*, 2012.
7. M.J. Gander, L. Halpern, and K. Santugini Repiquet. Discontinuous coarse spaces for DD-methods with discontinuous iterates. In *Domain Decomposition Methods in Science and Engineering XXI*, pages 607–615. Springer, 2014.
8. M.J. Gander, L. Halpern, and K. Santugini Repiquet. A new coarse grid correction for RAS/AS. In *Domain Decomposition Methods in Science and Engineering XXI*, pages 275–283. Springer, 2014.
9. M.J. Gander and A. Loneland. SHEM: An optimal coarse space for RAS and its multiscale approximation. In *Domain Decomposition Methods in Science and Engineering XXIII*. Springer, 2016.
10. M.J. Gander, A. Loneland, and T. Rahman. Analysis of a new harmonically enriched multiscale coarse space for domain decomposition methods. *arXiv preprint arXiv:1512.05285*, 2015.
11. A. Heinlein, A. Klawonn, J. Knepper, and O. Rheinbach. Multiscale coarse spaces for overlapping Schwarz methods based on the ACMS space in 2D. *ETNA*, 48:156–182, 2018.
12. A. Heinlein, A. Klawonn, J. Knepper, and O. Rheinbach. Adaptive GDSW coarse spaces for overlapping Schwarz methods in three dimensions. *SIAM J. Sci. Comput.*, 41(5):A3045–A3072, 2019.
13. C. Japhet. *Méthode de décomposition de domaine et conditions aux limites artificielles en mécanique des fluides : méthode optimisée d'ordre 2 (OO2)*. PhD thesis, Université Paris 13, 1998. http://www.theses.fr/1998PA132044.
14. A. Klawonn, M. Kuhn, and O. Rheinbach. Adaptive coarse spaces for FETI-DP in three dimensions. *SIAM J. Sci. Comput.*, 38(5):A2880–A2911, 2016.
15. Frédéric Nataf, Hua Xiang, Victorita Dolean, and Nicole Spillane. A coarse space construction based on local Dirichlet-to-Neumann maps. *SIAM J. Sci. Comput.*, 33(4):1623–1642, 2011.
16. N. Spillane, V. Dolean, P. Hauret, F. Nataf, C. Pechstein, and R. Scheichl. Abstract robust coarse spaces for systems of PDEs via generalized eigenproblems in the overlaps. *Numer. Math.*, 126(4):741–770, 2014.
17. A. Toselli and O. Widlund. *Domain decomposition methods-algorithms and theory*, volume 34. Springer Series in Computational Mathematics, 2005.